

On Generating Identifiable Virtual Faces

Zhuowen Yuan¹, Sheng Li^{1*}, Xinpeng Zhang¹, Zhenxin Qian¹, Alex Kot²

¹Fudan University

²Nanyang Technology University

{zwyuan18, lisheng, zhangxinpeng, zxqian}@fudan.edu.cn, eackot@ntu.edu.sg

Abstract

Face anonymization with generative models have become increasingly prevalent since they sanitize private information by generating virtual face images, ensuring both privacy and image utility. Such virtual face images are usually not identifiable after the removal or protection of the original identity. In this paper, we formalize and tackle the problem of generating identifiable virtual face images. Our virtual face images are visually different from the original ones for privacy protection. In addition, they are bound with new virtual identities, which can be directly used for face recognition. We propose an Identifiable Virtual Face Generator (IVFG) to generate the virtual face images. The IVFG projects the latent vectors of the original face images into virtual ones according to a user specific key, based on which the virtual face images are generated. To make the virtual face images identifiable, we propose a multi-task learning objective as well as a triplet styled training strategy to learn the IVFG. Various experiments demonstrate the effectiveness of the IVFG for generate identifiable virtual face images.

1 Introduction

Since the advent of the digital era, millions of images are shared over the Internet with the help of personal devices. Although they enable us to build stronger connections with the society, there is growing concern that these techniques may introduce privacy issues. Often, the images that are uploaded without sanitization contain privacy-sensitive information of individuals, such as identity, location, etc. Such private information may be leveraged by adversaries for malicious purposes. The public available images may also be collected and utilized to train machine learning models without consent (Harvey and LaPlace 2019).

To tackle these problems, obfuscation techniques such as pixelization and blurring (Hill et al. 2016) are widely adopted. However, these traditional methods fail to protect against modern attacks based on deep neural networks. McPherson *et al.* (McPherson, Shokri, and Shmatikov 2016) show that a trained attack model can re-identify the obfuscated face images with over 95% of accuracy. On the other hand, the quality of these obfuscated images are severely distorted, which could hardly be used for other computer

vision tasks. Recently, researchers propose to add adversarial noise to the face images (Shan et al. 2020; Raval, Machanavajhala, and Cox 2017) to mislead the face recognizer. These models rely on the prior knowledge of the face recognizer for high performance. People can easily reveal the original identity of the obfuscated face image by human perception (Li and Choi 2021).

A growing trend of researches take advantage of generative adversarial networks (GANs) (Goodfellow et al. 2014) for generating realistic face images from original face images (Maximov, Elezi, and Leal-Taixé 2020; Mirjalili, Raschka, and Ross 2020; Li and Choi 2021; Gu et al. 2020). One branch of these methods performs attribute editing while preserving the original identity. For instance, Mirjalili *et al.* (Mirjalili, Raschka, and Ross 2020) propose to remove sensitive soft attributes so that the generated faces can be used for face authentication, but the facial attributes can no longer be classified. These methods are not applicable when users require to protect the original identity from generated face images. Another category anonymizes the identity of the face image (Li and Choi 2021; Maximov, Elezi, and Leal-Taixé 2020; Mirjalili, Raschka, and Ross 2020), where the original identity is not revealed in the generated face images. Li and Choi (Li and Choi 2021) introduce an encoder-decoder network to perform perturbation on the latent space of GAN. The anonymized face image is generated from the perturbed latent vectors, which is visually different from the original face image. Despite the advantage, such anonymized face images cannot be used for authentication when needed.

In (Gu et al. 2020), the authors propose an approach to generate anonymized face images that can still be authenticated. They introduce a password conditioned model to generate the anonymized face images which could be decrypted into the original face images using the same password. As such, face authentication can be carried out in the original space after decryption. Obviously, the original identity is leaked to the third party who performs face authentication.

In this paper, we explore the possibility to generate identifiable virtual face images that satisfy the following requirements.

- The virtual face images are visually different from the original face images for anonymization.
- The virtual face images can be directly used for face au-

*Corresponding author.

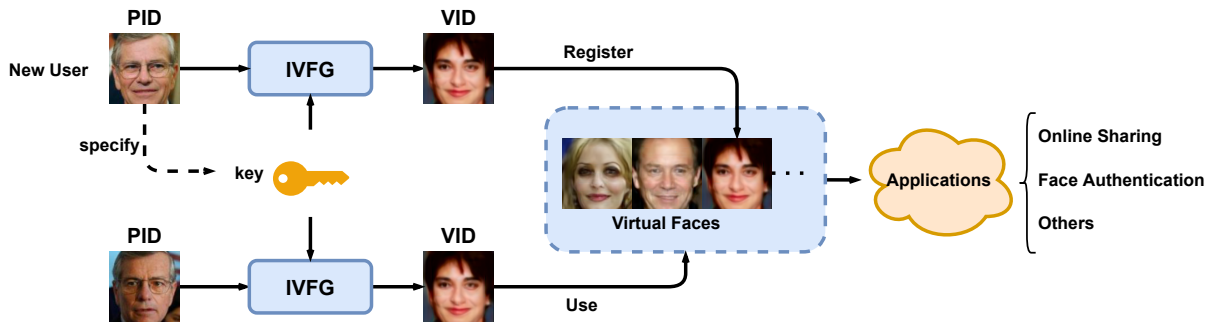


Figure 1: A typical application of our IVFG framework. Suppose that a user does not want to send his original face images to the untrusted applications, but still wishes to be identifiable. He can generate a virtual face image with our framework locally, and then feed the faces of his unique VID to the untrusted applications. Downstream applications are all performed in the virtual space, thus protecting the privacy of PIDs.

thentication in the virtual space.

Concretely, we propose a novel Identifiable Virtual Face Generator (IVFG) to fulfill such requirements. The IVFG maps an original face image into different virtual face images using different keys. For face images from the same original identity, the IVFG is able to generate virtual face images belonging to a unique virtual identity (VID) using a user specific key. In the following discussions, we also term the original identity as the physical identity (PID). The virtual face images can be used in different applications that require the face images as inputs for anonymization purpose. When face authentication is needed, we can submit the virtual faces and only the VID is used. As such, the PID is never leaked during the whole process, as shown in Fig. 1.

The main contributions are summarized below.

- We first explore the possibility to generate identifiable virtual face images which protects the PID and can be identified directly in the virtual space with off-the-shelf face recognizers.
- We propose a novel framework IVFG to map PIDs to VIDs conditioned on a user-specified key.
- We propose a multi-task learning objective as well as the corresponding training strategy to facilitate the training of IVFG.

The rest of the paper is organized as follows. Section 2 reviews recent advances in image obfuscation, generative models, and face anonymization. Section 3 formalizes the problem of generating identifiable virtual faces. Section 4 elaborates our proposed method in detail. Section 5 presents the experiment results, followed by the conclusions in the last section.

2 Related Work

In this section, we briefly summarize related work on image obfuscation, GANs, and face anonymization.

Image Obfuscation

Traditional methods such as pixelization, blurring (Hill et al. 2016) are widely adopted for image obfuscation.

These methods severely reduce the image quality and utility. They also fail to protect private information in images against deep models as already demonstrated by (McPherson, Shokri, and Shmatikov 2016). Another category of methods leverage the power of adversarial machine learning (Kurakin, Goodfellow, and Bengio 2017; Shan et al. 2020; Raval, Machanavajhala, and Cox 2017) to fool the classifier. Shan *et al.* (Shan et al. 2020) propose to add cloaks (i.e., adversarial noise) to the images. It achieves over 95 % protection rate even when the feature extractors of the user and the attacker are different. However, such obfuscated images are still recognizable by human perception (Li and Choi 2021). Raval *et al.* (Raval, Machanavajhala, and Cox 2017) jointly train an attacker network that learns to exploit secret information from the obfuscated images, and an obfuscator network that attempts to fool the attacker. This method relies on prior knowledge of the structure of the attacker’s model, which may not be applicable in many real-world scenarios.

Generative Adversarial Networks

The idea of GAN is initially introduced by (Goodfellow et al. 2014), which has widely been used for image generation. A typical GAN consists of a discriminator and a generator, which are jointly trained in a minimax game. The discriminator learns to distinguish between real and fake faces while the generator learns to generate realistic samples to fool the discriminator. Karras *et al.* (Karras, Laine, and Aila 2019) propose a style-based generator StyleGAN and achieve the state-of-the-art performance. Developments in GANs have also enabled controllable generation given input labels (Mirza and Osindero 2014). Abdal *et al.* (Abdal et al. 2021) investigate the latent space of StyleGAN and propose StyleFlow for attribute-conditioned semantic editing on projected real images. Richardson *et al.* (Richardson et al. 2021) propose an encoder for StyleGAN inversion, which demonstrates the possibility of face translation using pre-trained models. Various optimization strategies have been proposed (Arjovsky, Chintala, and Bottou 2017; Mao et al. 2017) to facilitate the training of GANs.

Face Anonymization

Face anonymization refers to publishing face images with the identity information sanitized. The image obfuscation techniques mentioned earlier can also be utilized for face anonymization. Recent advances take advantage of GAN to generate sanitized face images (Yan, Pei, and Nie 2019; Mirjalili, Raschka, and Ross 2020). Li and Lin (Li and Lin 2019) propose AnonymousNet that performs face attribute editing based on a set of privacy metrics. Similarly, Mirjalili *et al.* (Mirjalili, Raschka, and Ross 2020) propose to generate anonymized face images by removing sensitive soft attributes. These schemes only protect the privacy of the face attributes, the original identities (i.e., the PIDs) are preserved in the anonymized face images for authentication.

In order to protect the PIDs of the face images, Li and Choi (Li and Choi 2021) propose DeepBlur to perform blurring in the latent space of a pre-trained generative model, which is capable of synthesizing realistic face images with the PIDs removed. Maximov *et al.* (Maximov, Elezi, and Leal-Taixé 2020) propose a general face anonymization framework by mixing styles of different identities using GAN. The anonymized face images generated by such schemes cannot be utilized for authentication anymore due to the removal of PIDs. To deal with this issue, Gu *et al.* (Gu *et al.* 2020) propose a face image encryption framework to generate visually realistic encrypted face images based on different passwords. The encrypted face images well protect the PIDs, which can be decrypted into the original face images for authentication. Despite the advantage, this method fails to protect the PIDs after the face image decryption, and the protection mainly relies on the secrecy of the password.

In this paper, we propose to generate identifiable virtual face images for anonymization. The virtual face images are generated based on both the original face image and a user specific key. Unlike the work in (Gu *et al.* 2020), our virtual faces can be authenticated directly in the virtual space without leaking the PIDs.

3 Problem Formulation

Let \mathcal{X} and \mathcal{Y} denote two sets of face images, where images within each set belong to the same person (i.e., the same PID). The anonymization process is conditioned on a user-specified key $k \in \mathcal{K}$. We further denote $T(x, k)$ as the virtual face image generated from the original face image x and key k , and $I(x)$ as the identity that can be extracted from x .

Given the original face images $x_1, x_2 \in \mathcal{X}$, $y \in \mathcal{Y}$ and two disparate keys $k_1, k_2 \in \mathcal{K}$, our goal is to generate virtual face images that meet the following properties.

Property 1 (Anonymization) *The original face image and virtual face image should belong to different identities, namely $VID \neq PID$.*

$$I(T(x_1, k_1)) \neq I(x_1) \quad (1)$$

Property 2 (Diversity) *The key controls the VID of the anonymized face images, i.e., the virtual face images of the same PID belong to different VIDs under different keys.*

$$I(T(x_1, k_1)) \neq I(T(x_1, k_2)) \quad (2)$$

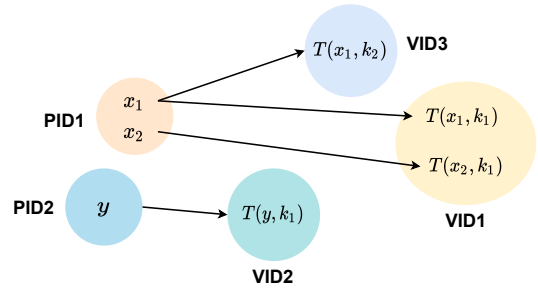


Figure 2: An anonymization system that conforms to the properties formulated in section 3. The arrows represent anonymization processes.

Property 3 (Identifiability) *Given two original face images belonging to the same PID, the corresponding virtual face images should belong to the same VID under the same key.*

$$I(T(x_1, k_1)) = I(T(x_2, k_1)) \quad (3)$$

Property 4 (Separability) *Given two original face images belonging to different PIDs, the corresponding virtual face images should belong to different VIDs under the same or different keys.*

$$\begin{aligned} I(T(x_1, k_1)) &\neq I(T(y, k_1)) \\ I(T(x_1, k_1)) &\neq I(T(y, k_2)) \end{aligned} \quad (4)$$

Fig. 2 illustrates the aforementioned properties intuitively.

4 Methodology

In this section, we introduce our IVFG framework, learning objective and training strategy.

The Proposed Framework

The overall structure of our proposed IVFG framework is illustrated in Fig. 3(a). The IVFG framework is based on an encoder-decoder architecture, which is composed of three modules: an encoder E , a latent projector P and a face generator G . The encoder E takes an image tensor x as input and outputs the extracted facial representation, say r . We propose a latent projector P to project the combination of facial representation r and key k to the latent space of the generator, which is composed of a concatenation operation and a multilayer perceptron (MLP). We use the generator of a pre-trained GAN as our G , which maps a vector in latent space $z \in \mathcal{Z}$ to realistic images from the distribution of training data $x \sim p(x)$, namely: $G : z \mapsto x$.

Learning Objective

We design a multi-task learning objective to satisfy the four properties mentioned in Section 3 for training the IVFG. We leverage the following cosine embedding loss \mathcal{L}_{emb} to measure the similarity between two facial features f_1 and f_2 , where

$$\mathcal{L}_{emb}(f_1, f_2, l) = \begin{cases} 1 - \cos(f_1, f_2), & l = 1 \\ \max(m, \cos(f_1, f_2)), & l = -1 \end{cases} \quad (5)$$

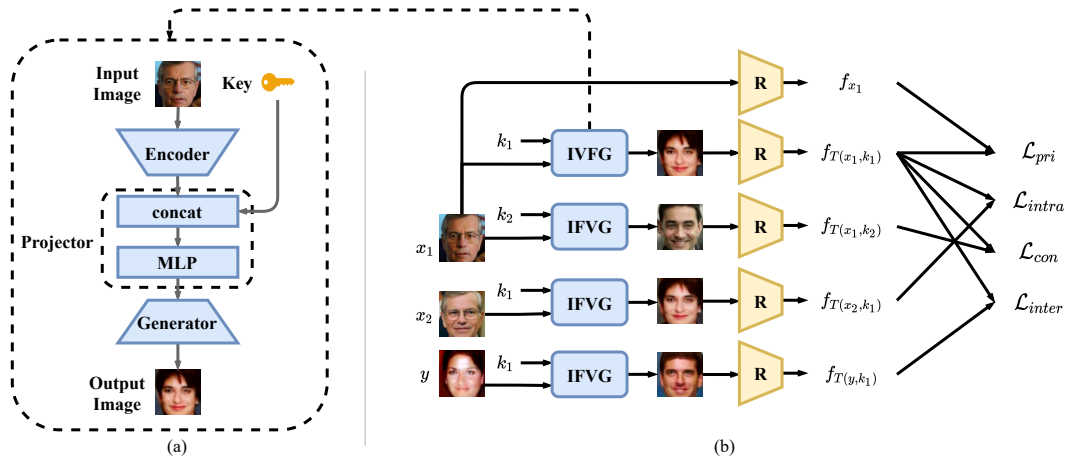


Figure 3: (a) The proposed IVFG framework. (b) Overview of our training strategy.

where \cos denotes cosine similarity, m is a hyperparameter, and l is the identity indicator. $l = 1$ refers to the case that f_1 and f_2 to be from the same identity, and we are pushing f_1 and f_2 to be close to each other by optimizing \mathcal{L}_{emb} . On the contrary, we try to separate f_1 and f_2 to make them belong to different identities if l is set to -1 .

Privacy Loss. To satisfy Property 1, we propose privacy loss \mathcal{L}_{pri} to modify the identity of the original face image. In other words, \mathcal{L}_{pri} guides the anonymization process so that $PID \neq VID$, where

$$\mathcal{L}_{pri} = \mathbb{E}_{\mathcal{X}, \mathcal{K}}[\mathcal{L}_{emb}(R(T(x_1, k_1)), R(x_1), -1)] \quad (6)$$

where $R(x)$ extracts the features from the face image x .

Conditional Loss. To satisfy Property 2, we propose conditional loss \mathcal{L}_{con} to make sure that the generated virtual identity can be controlled by a user-specified key. Given two different keys k_1, k_2 and an original face image, the model should be able to generate two distinct VIDs by using \mathcal{L}_{con} below.

$$\mathcal{L}_{con} = \mathbb{E}_{\mathcal{X}, \mathcal{K}}[\mathcal{L}_{emb}(R(T(x_1, k_1)), R(T(x_1, k_2)), -1)] \quad (7)$$

Intra-group Classification Loss. To satisfy Property 3, we have to guarantee that, given two original face images from the same PID: $x_1, x_2 \in \mathcal{X}$, the corresponding virtual face images generated using same key should belong to the same VID. Therefore, the intra-group classification loss is formulated as

$$\mathcal{L}_{intra} = \mathbb{E}_{\mathcal{X}, \mathcal{K}}[\mathcal{L}_{emb}(R(T(x_1, k_1)), R(T(x_2, k_1)), 1)] \quad (8)$$

Inter-group Classification Loss. To satisfy Property 4, we propose the following inter-group classification loss \mathcal{L}_{inter} to maximize the distance between VIDs that are generated from different PIDs

$$\mathcal{L}_{inter} = \mathbb{E}_{\mathcal{X}, \mathcal{Y}, \mathcal{K}}[\mathcal{L}_{emb}(R(T(x_1, k_1)), R(T(y, k_1)), -1)], \quad (9)$$

where x and y are face images from different PIDs.

Regularization. With the above losses, the predicted latent vectors may deviate from the latent space of G , leading to

non-convergence. To deal with this issue, we further propose a regularization term to bound the distribution of the projected latent vectors such that they are within the latent space of G . Specifically, we first calculate the mean latent vector \bar{z} by sampling m latent vectors z_1, z_2, \dots, z_m from the latent distribution of G . Then, we minimize the L2 distance between the predicted latent vector z and \bar{z} .

$$\mathcal{L}_{reg} = \|z - \bar{z}\|_2^2 \quad (10)$$

Our full objective is a weighted average over the above mentioned loss functions, which is given below.

$$\mathcal{L} = \lambda_{pri}\mathcal{L}_{pri} + \lambda_{con}\mathcal{L}_{con} + \lambda_{intra}\mathcal{L}_{intra} + \lambda_{inter}\mathcal{L}_{inter} + \lambda_{reg}\mathcal{L}_{reg} \quad (11)$$

Training Strategy

During training, we leverage an auxiliary face recognizer R for facial feature extraction. We use pre-trained models for E, G, R whose parameters will be frozen in the training. We only update the parameters of P by

$$P^* = \arg \min_P \mathcal{L}. \quad (12)$$

We split the dataset \mathcal{S} into triplets of images. For each triplet $s \in \mathcal{S}$, we have $s = \{x_1, x_2, y\}$ with x_1, x_2 belonging to the same PID and y for another PID. Given two different keys k_1 and k_2 , we can derive a quaternion s' of four virtual images: $s' = \{T(x_1, k_1), T(x_1, k_2), T(x_2, k_1), T(y, k_1)\}$. Then, we calculate the objective function and perform back propagation. Such a triplet styled training strategy is illustrated in Fig. 3(b) with the details given in Algorithm 1.

5 Experiments

Dataset

Our model is trained and evaluated on LFW (Huang et al. 2007). The dataset consists of 13,233 face images of 5,749 unique identities, including 1,680 identities with two or more images. We perform an 8:1:1 split based on identities for training, validation, and testing. Then, we split the each

Algorithm 1: IVFG Training

Input: E : pre-trained encoder; G : pre-trained generator; R : pre-trained face recognizer; $P(f, k; W)$: latent projector; W : parameters of P , \mathcal{S}_n : dataset containing n triplets

Parameter: $\lambda_{pri}, \lambda_{con}, \lambda_{intra}, \lambda_{inter}, \lambda_{reg}$: weights for the training objective; α : learning rate

```
1: Freeze  $E, G, R$ .
2: // Generate  $\hat{z}$  by sampling from latent space.
3:  $z_1, \dots, z_m = \text{sample}(z), z \sim p(z)$ 
4:  $\hat{z} = \frac{1}{m} \sum_{j=1}^m z_j$ 
5: for  $i \leftarrow 1$  to  $n$  do
6:    $k_1, k_2 \leftarrow \text{generate two distinct keys}$ 
7:    $x_1, x_2, y \leftarrow \mathcal{S}_i$ 
8:    $r_{x_1} \leftarrow E(x_1)$  // Extract facial representations.
9:    $r_{x_2} \leftarrow E(x_2)$ 
10:   $r_y \leftarrow E(y)$ 
11:   $z_{x_1, k_1} \leftarrow P(r_{x_1}, k_1; W_i)$  // Project to latent vectors.
12:   $z_{x_1, k_2} \leftarrow P(r_{x_1}, k_2; W_i)$ 
13:   $z_{x_2, k_1} \leftarrow P(r_{x_2}, k_1; W_i)$ 
14:   $z_{y, k_1} \leftarrow P(r_y, k_1; W_i)$ 
15:   $T(x_1, k_1) \leftarrow G(z_{x_1, k_1})$  // Generate virtual faces.
16:   $T(x_1, k_2) \leftarrow G(z_{x_1, k_2})$ 
17:   $T(x_2, k_1) \leftarrow G(z_{x_2, k_1})$ 
18:   $T(y, k_1) \leftarrow G(z_{y, k_1})$ 
19:  Calculate full objective  $\mathcal{L}$  from Eq. 11.
20:   $\nabla W_i = \partial \mathcal{L} / \partial W_i$ 
21:   $W_{i+1} = W_i - \alpha \nabla W_i$ 
22: end for
23: return  $W_{i+1}$ 
```

set into triplets of images as discussed in the previous section. All face images are aligned and cropped to 128×128 by MTCNN (Zhang et al. 2016).

Implementation Details

We use FaceNet Inception-ResNet-v1 (Szegedy et al. 2017) for both E and R during training. Both of them are pre-trained on VGGFace2 (Cao et al. 2018). For the input key, we use an n -digit binary number, which is represented by a n -dimensional vector $k \in \{0, 1\}^n$. We set n to 8 as default value. G is a StyleGAN (Karras, Laine, and Aila 2019) generator trained from scratch on LFW with progressive growing (Karras et al. 2018). We stop after the 128-pixel training step since we only use the model for generating 128×128 images. For effective and stable evaluation, all noises included in the original StyleGAN implementation are cancelled during both training and evaluating. Our projector P maps the concatenation of facial representation and key into the intermediate latent space \mathcal{W} of StyleGAN instead of Z since \mathcal{W} achieves better disentanglement as pointed out by (Karras, Laine, and Aila 2019). $w \in \mathcal{W}$ directly controls the generator through adaptive instance normalization (Huang and Belongie 2017) at each convolution layer. We set the number of hidden layers of the MLP in P to 2.

We set $\lambda_{pri} = 0.1$, $\lambda_{con} = 1$, $\lambda_{intra} = 1$, $\lambda_{inter} = 1$, $\lambda_{reg} = 20$ based on quantitative observations. We set the identity indicator l in cosine embedding loss to 0.4. We train

the model for 20 epochs with the Adam optimizer (Kingma and Ba 2017), where $\beta_1 = 0.9$ and $\beta_2 = 0.999$. Learning rate is set to 3×10^{-4} . The training process takes only 1 hour on a single NVIDIA GTX 1080Ti GPU.

Performance

We evaluate the performance of our virtual face images with a pre-trained face recognizer R . To demonstrate that our framework is scalable, we use a different architecture for R during evaluating. Specifically, we use SphereFace (Liu et al. 2017) which is pre-trained on CASIA-WebFace (Yi et al. 2014). We denote the threshold of the EER for the this pre-trained model on the LFW dataset as t_{eer} which is 0.36. To the best of our knowledge, we are the first to propose and formalize the task of generating identifiable virtual face images. Here, we compare the performance of our method with the most relevant work proposed by Gu et al. (Gu et al. 2020), which is able to generate real-look alike encrypted face images using different keys.

Face Recognition In this section, we evaluate the performance of our virtual faces in terms of face recognition, including Equal Error Rate (EER) and Area Under Curve (AUC). We generate the following two sets of virtual face images from the LFW dataset:

- Set-A: We assign a unique key to different identities to generate the virtual face images.
- Set-B: Each identity is assigned with the same key to generate the virtual face images.

Set-A refers to the case that the user specific key is not known by the adversary, while Set-B is generated for evaluating the key-stolen case. On both sets, we generate the same sets of virtual face images using the method proposed in (Gu et al. 2020) for comparison. Table 1 gives the EER and AUC for different sets of face images, where ‘original’ refers to the set of the original face images. It can be seen that, our virtual face images achieve the best recognition performance when the key is well protected, which is even better than that of the original face images. When the key is stolen, the EER drops around 8% using our virtual face images.

Next, we use the virtual face images in Set A and the corresponding keys for input and run the IVFG again to generate a set of recovered face images. We match these recovered face images with the original face images, the successful match rate of which is 0 ± 0.001 at the EER threshold t_{eer} . This is to say, it is difficult to recover the original face images when our virtual face image, the key and the trained IVFG are compromised. While in (Gu et al. 2020), the original face image can be directly decrypted from the encrypted face image using the correct password.

Anonymization We evaluate the anonymization performance of our virtual face images in terms of protection rate, which is computed as the unsuccessful match rate between the original and anonymized face images. Specifically, we match the original face image and the corresponding anonymized face image. If the match score is less than t_{eer} , these two images are considered to be from different identities and an unsuccessful match is yielded. Table

Methods	EER	AUC
Original	0.024	0.998
Gu et al. (Set-A)	0.105±0.009	0.957±0.004
Gu et al. (Set-B)	0.136±0.012	0.929±0.006
Ours (Set-A)	0.018±0.005	0.999±0.001
Ours (Set-B)	0.103±0.009	0.963±0.004

Table 1: Face recognition performance on different image sets.

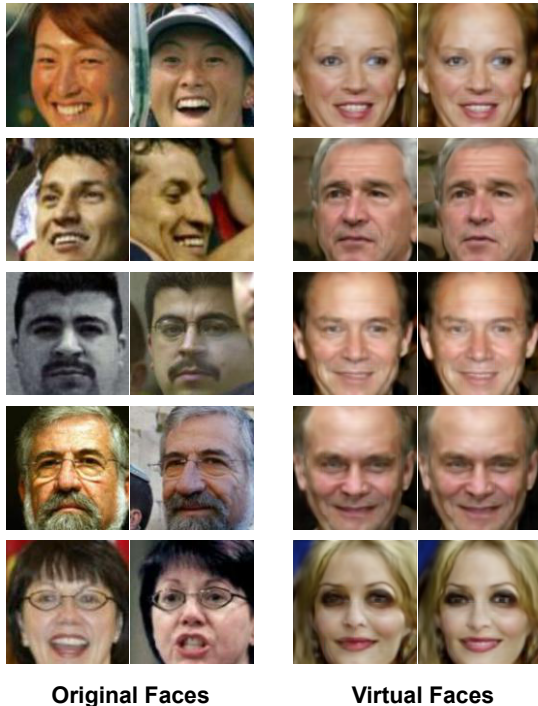


Figure 4: Examples of our virtual face images. The first two images in each row are the original faces images, while the third and fourth images are the virtual face images of the first and second images, respectively.

2 reports the protection rate of our virtual face images and Gu et al.’s encrypted face images on the test set of LFW. It can be seen that our virtual face images offer excellent anonymization with protection rate of 0.988, which is significantly better than Gu et al.’s method.

Diversity We evaluate here how different virtual face images could be generated using different keys. For each face image from the test set of LFW, we use two different keys to generate two virtual face images. We match these two virtual face images to see if the matching is successful (i.e., the matching score is over t_{eer}). The diversity is measured as the unsuccessful match rate among the virtual face images generated using different keys, the results of which is given in Table 2. It can be seen that our method performs significantly better than (Gu et al. 2020) in terms of diversity.

Metrics	Gu et al.	Ours
Protection Rate	0.052±0.007	0.988±0.005
Diversity	0.008±0.003	0.750±0.013

Table 2: Performance on anonymization and diversity.



Figure 5: Diverse virtual face images generated from the same original face image with different keys. In each row, the first image is the original images, the rest images are the corresponding virtual face images generated using different keys.

Visual Quality To evaluate the visual quality of the virtual face images, we report the detection rate using the *state-of-the-art* face detector MTCNN (Zhang et al. 2016) as well as the Fréchet Inception Distance (FID) (Heusel et al. 2018) to quantify the similarity of data distributions between the virtual face images and real ones. The face detection thresholds using MTCNN are set as the default values. Table 4 gives the results for our proposed method, Gu et al.’s method and traditional methods including pixelization (with pixel size of 18) and blurring (Gaussian blur with kernel size of 37 and $\sigma=6$). Our method achieves perfect detection rate of 1.0. In terms of FID, our method significantly outperforms traditional anonymization methods and achieves comparable results with (Gu et al. 2020).

Fig. 4 gives a few examples of our virtual face images as well as the corresponding original ones. Fig. 5 further illustrates the diverse virtual face images that are generated from the same original face image with different keys.

Feature Space Visualization

In this section, we visualize the feature space of the original and virtual face image for qualitative analysis. We randomly select 10 identities from LFW with at least 30 face images, from which we generate different sets of virtual face images using different keys (i.e., Set A) or the same key (i.e., Set B). We perform t-SNE on the extracted facial features of the original and virtual faces (Van der Maaten and Hinton 2008) in Set A and Set B, the visualization results of which is shown in Fig. 6. We can see that in the case of different keys (i.e., Set A), the virtual facial features are more sparsely

Methods	Protection Rate	Diversity	EER (same key)	EER (different keys)	FID
w/o \mathcal{L}_{pri}	0.978 \pm 0.006	0.718 \pm 0.010	0.105 \pm 0.008	0.021 \pm 0.009	6.066 \pm 0.056
w/o \mathcal{L}_{con}	0.987 \pm 0.003	0.0 \pm 0.0	0.108 \pm 0.005	0.096 \pm 0.004	7.641 \pm 0.008
w/o \mathcal{L}_{intra}	0.968 \pm 0.008	0.764 \pm 0.019	0.190 \pm 0.008	0.112 \pm 0.008	5.776 \pm 0.086
w/o \mathcal{L}_{inter}	0.982 \pm 0.004	0.803 \pm 0.015	0.180 \pm 0.012	0.0 \pm 0.0	6.339 \pm 0.037
w/o \mathcal{L}_{reg}	0.996 \pm 0.002	0.740 \pm 0.021	0.096 \pm 0.007	0.016 \pm 0.005	15.535 \pm 0.144
full objective	0.988 \pm 0.005	0.750 \pm 0.013	0.103 \pm 0.009	0.018 \pm 0.005	6.170 \pm 0.050

Table 3: Ablation study of our model. From the second row, each row shows the performance of our framework with one loss component removed.

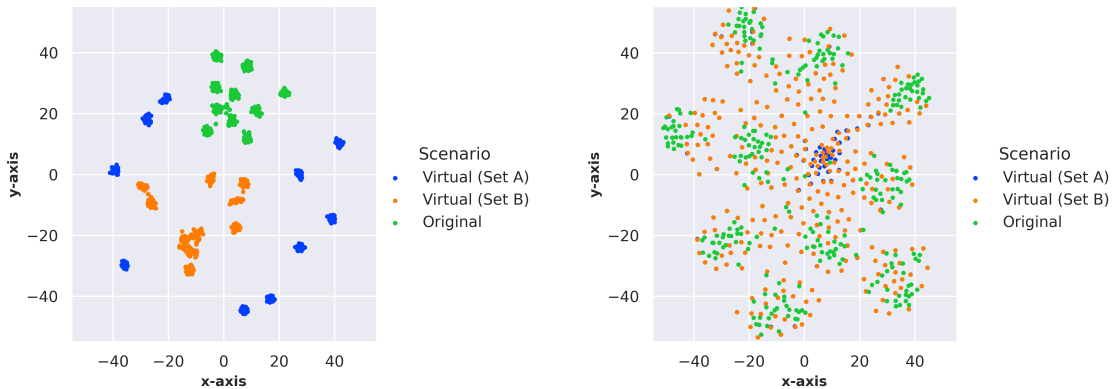


Figure 6: t-SNE visualization of the feature space of different face image sets, left: ours, right: Gu et al.’s

Methods	Detection	FID
Pixelization	0.984	44.451
Blurring	0.991	62.786
Gu et al.	1.0 \pm 0.001	4.782 \pm 0.027
Ours	1.0 \pm 0.0	6.170 \pm 0.050

Table 4: Detection rate and FID scores between the original and anonymized faces. The scores are calculated on features from the second max pooling layer. The dimensionality of features is 192.

distributed than the original ones, which can be well classified in the virtual space. On the other hand, the features of our virtual face images can also be well separated from the original ones, leading to good anonymization ability. When the key is stolen (Set B), the virtual features are still clustered to a certain extent. We also compare our virtual feature space with that of Gu et al.’s. It can be seen that, by using Gu et al.’s method, the features of the encrypted face images are not well clustered, which are also difficult to be differentiated from the original ones.

Ablation Study

In this section, we present ablation studies to demonstrate the effectiveness of each loss component in our multi-task learning objective. We remove each loss component from the overall training objective separately and report the re-

sults in Table 3.

It can be seen from Table 3 that the \mathcal{L}_{pri} effectively pushes the features apart, the protection rate drops if \mathcal{L}_{pri} is removed. Moreover, the average cosine similarity drops from 0.0052 to 0.0024 between virtual and original facial features when \mathcal{L}_{pri} is incorporated during training. Without \mathcal{L}_{con} , the model fails to be conditioned on the user-specified key to generate different virtual face images. The results of w/o \mathcal{L}_{intra} and w/o \mathcal{L}_{inter} demonstrate that both the intra-group and inter-group classification losses are necessary for high face recognition accuracy. The results of w/o \mathcal{L}_{reg} shows that \mathcal{L}_{reg} regularizes the anonymization process to produce realistic face images.

6 Conclusions

In this paper, we propose and formalize a novel task in face anonymization: generating identifiable virtual face images. To this end, we propose a framework termed as the IVFG for the generation of identifiable virtual face images. The input of the IVFG is the original face image and a user specific key, the output is a virtual face image bound with a unique virtual identity. Our virtual face images are visually different from the original ones for protecting the original identity, which could also be directly recognized in the virtual space for authentication. We also propose a multi-task learning objective and a triplet styled training strategy to effectively train the IVFG. Experimental results demonstrate that our virtual face images achieve good performance in terms of anonymization and the identification of virtual identities.

References

- Abdal, R.; Zhu, P.; Mitra, N. J.; and Wonka, P. 2021. Styleflow: Attribute-conditioned exploration of stylegan-generated images using conditional continuous normalizing flows. *ACM Transactions on Graphics (TOG)*, 40(3): 1–21.
- Arjovsky, M.; Chintala, S.; and Bottou, L. 2017. Wasserstein GAN. arXiv:1701.07875.
- Cao, Q.; Shen, L.; Xie, W.; Parkhi, O. M.; and Zisserman, A. 2018. Vggface2: A dataset for recognising faces across pose and age. In *2018 13th IEEE international conference on automatic face & gesture recognition (FG 2018)*, 67–74. IEEE.
- Goodfellow, I.; Pouget-Abadie, J.; Mirza, M.; Xu, B.; Warde-Farley, D.; Ozair, S.; Courville, A.; and Bengio, Y. 2014. Generative adversarial nets. *Advances in neural information processing systems*, 27.
- Gu, X.; Luo, W.; Ryoo, M. S.; and Lee, Y. J. 2020. Password-conditioned anonymization and deanonymization with face identity transformers. In *European Conference on Computer Vision*, 727–743. Springer.
- Harvey, A.; and LaPlace, J. 2019. MegaPixels: origins, ethics, and privacy implications of publicly available face recognition image datasets. *Megapixels*.
- Heusel, M.; Ramsauer, H.; Unterthiner, T.; Nessler, B.; and Hochreiter, S. 2018. GANs Trained by a Two Time-Scale Update Rule Converge to a Local Nash Equilibrium. arXiv:1706.08500.
- Hill, S.; Zhou, Z.; Saul, L. K.; and Shacham, H. 2016. On the (In) effectiveness of Mosaicing and Blurring as Tools for Document Redaction. *Proc. Priv. Enhancing Technol.*, 2016(4): 403–417.
- Huang, G. B.; Ramesh, M.; Berg, T.; and Learned-Miller, E. 2007. Labeled Faces in the Wild: A Database for Studying Face Recognition in Unconstrained Environments. Technical Report 07-49, University of Massachusetts, Amherst.
- Huang, X.; and Belongie, S. 2017. Arbitrary style transfer in real-time with adaptive instance normalization. In *Proceedings of the IEEE International Conference on Computer Vision*, 1501–1510.
- Karras, T.; Aila, T.; Laine, S.; and Lehtinen, J. 2018. Progressive Growing of GANs for Improved Quality, Stability, and Variation. arXiv:1710.10196.
- Karras, T.; Laine, S.; and Aila, T. 2019. A style-based generator architecture for generative adversarial networks. In *Proceedings of the IEEE/CVF Conference on Computer Vision and Pattern Recognition*, 4401–4410.
- Kingma, D. P.; and Ba, J. 2017. Adam: A Method for Stochastic Optimization. arXiv:1412.6980.
- Kurakin, A.; Goodfellow, I.; and Bengio, S. 2017. Adversarial examples in the physical world. arXiv:1607.02533.
- Li, T.; and Choi, M. S. 2021. DeepBlur: A Simple and Effective Method for Natural Image Obfuscation. arXiv:2104.02655.
- Li, T.; and Lin, L. 2019. Anonymousnet: Natural face de-identification with measurable privacy. In *Proceedings of the IEEE/CVF Conference on Computer Vision and Pattern Recognition Workshops*, 0–0.
- Liu, W.; Wen, Y.; Yu, Z.; Li, M.; Raj, B.; and Song, L. 2017. SpheroFace: Deep hypersphere embedding for face recognition. In *Proceedings of the IEEE conference on computer vision and pattern recognition*, 212–220.
- Mao, X.; Li, Q.; Xie, H.; Lau, R. Y.; Wang, Z.; and Paul Smolley, S. 2017. Least squares generative adversarial networks. In *Proceedings of the IEEE international conference on computer vision*, 2794–2802.
- Maximov, M.; Elezi, I.; and Leal-Taixé, L. 2020. Ciagan: Conditional identity anonymization generative adversarial networks. In *Proceedings of the IEEE/CVF Conference on Computer Vision and Pattern Recognition*, 5447–5456.
- McPherson, R.; Shokri, R.; and Shmatikov, V. 2016. Defeating Image Obfuscation with Deep Learning. arXiv:1609.00408.
- Mirjalili, V.; Raschka, S.; and Ross, A. 2020. PrivacyNet: semi-adversarial networks for multi-attribute face privacy. *IEEE Transactions on Image Processing*, 29: 9400–9412.
- Mirza, M.; and Osindero, S. 2014. Conditional Generative Adversarial Nets. arXiv:1411.1784.
- Raval, N.; Machanavajjhala, A.; and Cox, L. P. 2017. Protecting visual secrets using adversarial nets. In *2017 IEEE Conference on Computer Vision and Pattern Recognition Workshops (CVPRW)*, 1329–1332. IEEE.
- Richardson, E.; Alaluf, Y.; Patashnik, O.; Nitzan, Y.; Azar, Y.; Shapiro, S.; and Cohen-Or, D. 2021. Encoding in style: a stylegan encoder for image-to-image translation. In *Proceedings of the IEEE/CVF Conference on Computer Vision and Pattern Recognition*, 2287–2296.
- Shan, S.; Wenger, E.; Zhang, J.; Li, H.; Zheng, H.; and Zhao, B. Y. 2020. Fawkes: Protecting privacy against unauthorized deep learning models. In *29th {USENIX} Security Symposium ({USENIX} Security 20)*, 1589–1604.
- Szegedy, C.; Ioffe, S.; Vanhoucke, V.; and Alemi, A. A. 2017. Inception-v4, inception-resnet and the impact of residual connections on learning. In *Thirty-first AAAI conference on artificial intelligence*.
- Van der Maaten, L.; and Hinton, G. 2008. Visualizing data using t-SNE. *Journal of machine learning research*, 9(11).
- Yan, B.; Pei, M.; and Nie, Z. 2019. Attributes Preserving Face De-Identification. In *ICCV Workshops*, 1217–1221.
- Yi, D.; Lei, Z.; Liao, S.; and Li, S. Z. 2014. Learning Face Representation from Scratch. arXiv:1411.7923.
- Zhang, K.; Zhang, Z.; Li, Z.; and Qiao, Y. 2016. Joint face detection and alignment using multitask cascaded convolutional networks. *IEEE Signal Processing Letters*, 23(10): 1499–1503.